

Vibrational studies on CO₂ up to 40 GPa by Raman spectroscopy at room temperature

H. Olijnyk and A. P. Jephcoat

Department of Earth Sciences, University of Oxford, Oxford OX1 3PR, United Kingdom

(Received 3 July 1997)

Raman spectra of CO₂ were obtained under hydrostatic (in He-N₂) and nonhydrostatic (pure CO₂) pressures up to 40 GPa at room temperature. The pressure-induced changes of the librational spectra suggest that solid CO₂ does not transform directly from phase I (cubic *Pa3*) to phase III (orthorhombic *Cmca*). An intermediate phase IV, which may involve only minor modifications of phase I, is formed prior to the transition to *Cmca* structure. Phases IV and III coexist over some pressure range. The pressure shifts of all four Raman-active librations of phase III were determined over a wide pressure range and are compared to previous theoretical results. Splittings in the ν^- and ν^+ modes are observed in the stability field of phase I below 10 GPa. The frequency of the ν^+ mode decreased slightly whereas the frequency of the ν^- mode increased slightly at the transition to phase III. The liquid-to-solid transition at 0.6 GPa was confirmed. [S0163-1829(98)04502-0]

INTRODUCTION

CO₂ is an important volatile component of the earth as well as other planets in the solar system. Its high-pressure behavior is therefore of fundamental importance in planetary science. On condensation into the solid state CO₂ forms a simple molecular crystal. The crystalline structure of such solids is mainly determined by weak intermolecular interactions, while the molecule itself is held together by strong intramolecular forces. High-pressure spectroscopic studies provide useful data for refining the various model potentials which are used for the prediction of the physical properties of such systems as well as for the formation of different phases.

The liquid-to-solid transition was reported¹⁻³ to occur at 0.5–0.6 GPa at room temperature. In the solid state, CO₂ crystallizes in a fcc lattice (space group *Pa3*), with the molecular axes oriented along the body diagonals of the cubic cell. Indications for another phase II between 0.5 and 2.3 GPa at room temperature from high-pressure x-ray-diffraction studies by Liu⁴ could not be verified by the x-ray-diffraction studies by Olinger⁵ and the Raman studies by Hanson and Jones,⁶ which confirmed that CO₂ remains stable in the cubic phase up to at least ~ 10 GPa. While the x-ray-diffraction studies of Liu⁷ revealed no phase changes in the pressure range up to 50 GPa, Hanson⁸ observed a new high-pressure phase III above 18 GPa in a subsequent room-temperature Raman study up to 25 GPa by drastic changes of the spectral features in the low-frequency region. This transition was confirmed by Raman studies at low temperatures⁹ with the transition pressure around 11 GPa and large hysteresis. In this study indications for the formation of an additional phase IV prior to the transition to phase III were found in the librational Raman spectra. On the basis of free-energy calculations, Kuchta and Etters¹⁰⁻¹² predicted an orthorhombic structure (*Cmca*) for the high-pressure phase III and calculated transition pressures are 4.3 GPa for 0 K and 11 GPa for room temperature. This structural assignment was later questioned by the results of infrared and Raman spectroscopic studies by Aoki, Yamawaki, and Sakashita,¹³ who instead suggested a tetragonal lattice isomorphous with γ -N₂ as a more likely candidate for the high-pressure phase. How-

ever, from subsequent x-ray-diffraction studies Aoki *et al.*¹⁴ concluded that an orthorhombic *Cmca* structure supersedes the low-pressure cubic phase above about 10 GPa. A more recent infrared study¹⁵ of librations up to 50 GPa has been reported to be compatible with a *Cmca* structure for the high-pressure phase and no indications of a phase IV were detected.

The reported transition pressures^{8,9,13-15} range from 10 to 18 GPa on loading and are some GPa lower on unloading at room temperature and also depend on the pressure history of the specimen. Another reported feature of the phase transition is the coexistence of phases I and III over a wide pressure range.¹⁵

In the orthorhombic structure, the originally equivalent cubic axes split into the orthorhombic *a*, *b*, and *c* axes, and at the same time the molecules tilt down on one of the base planes with their molecular axes inclined at 52° from the *c* axes.¹⁴ Comparison between experimental and theoretical lattice parameters shows good agreement for the *b* and *c* axes, but is far less satisfactory for the *a* axes, which has been attributed to an insufficient theoretical description of the intermolecular interactions along the *a* axes.¹⁴ Another test of the intermolecular interactions is provided by the librational Raman shifts and their pressure dependences. The *Cmca* phase supports four Raman-active librational modes. Previous Raman spectroscopic results^{8,9,13} led to contradictory results regarding the number of observed Raman librations. Aoki, Yamawaki, and Sakashita¹³ reported two whereas Hanson⁸ observed three low-frequency Raman modes. It was, however, conjectured that the strongest of these lines could be in fact two separately unresolved lines.⁹ The calculated librational modes compare reasonably well with the existing experimental data.¹⁰

One difficulty in high-pressure studies on CO₂ is the appearance of large pressure inhomogeneities in the high-pressure phase. For example, Hanson⁸ reported differences of 5 GPa or larger within the sample for phase III, which makes it difficult to obtain Raman spectra of satisfactory quality at higher pressures and might account for the contradictory results of previous Raman studies.

In the present Raman study of CO₂ the pressure range was extended up to 40 GPa, as compared to 25 GPa for the

librons^{6,8,9,13} and 18 GPa for the vibrons^{6,9} in previous studies. By using a quasihydrostatic pressure transmitting medium we have been able to overcome the problem of poor quality Raman spectra due to pressure inhomogeneities and provide evidence for the existence of a phase IV (Ref. 9) and confirm the existence of four Raman-active librational modes in phase III.

EXPERIMENT

In one run CO₂ was used as the sample and pressure transmitting medium at the same time (nonhydrostatic conditions). In a second run, a gas mixture of 7% CO₂, 18% N₂, and 75% He was used. In this system, CO₂ freezes out at 1.5 GPa, and the remaining He-N₂ mixture, which becomes solid around 9 GPa, and excess He, which becomes solid around 12 GPa, serve as a pressure-transmitting medium for CO₂ (quasihydrostatic conditions). The pressure distribution across the sample chamber was determined at various pressures. We found no pressure differences within experimental error at 16.8 GPa and only minor differences of 1 GPa over the total gasket hole were noticed at 30.8 GPa. Measurements of the ruby linewidth and ruby $R_1 - R_2$ splitting indicate that quasihydrostatic conditions were maintained at the highest pressures. The gases were filled into the gasket hole of a high-pressure diamond-anvil cell at 0.2 GPa using a high-pressure gas-loading technique.¹⁶ Raman spectra were excited by the 514.5 nm line of an Ar⁺ laser, which was focused to 20 μ m on the sample. Scattered light, collected through a spatial filtering aperture, was analyzed at an angle of 135° with respect to the incoming laser beam using a 0.6 m triple spectrograph and a liquid-nitrogen-cooled CCD multichannel detector. Pressure was determined with the ruby fluorescence method.¹⁷

SPECTRAL FEATURES

The primitive unit cell of the cubic phase contains four CO₂ molecules. According to symmetry selection rules the Raman spectrum in the low-frequency region consists of three librational modes. From the three internal vibrations of the CO₂ molecule only the symmetric stretch should be Raman active. The crystal field splits the symmetric stretch ν_1 into a threefold degenerate F_g mode and an A_g mode.¹⁸ Due to Fermi resonance (FR) between the symmetric stretch mode ν_1 and two-phonon states of the bending mode ν_2 further modifications in the spectral features occur. In the case of CO₂, two bound states, usually denoted as ν^+ and ν^- to emphasize the effect of FR, separate as intense peaks from both sides of the two-phonon states.¹⁹ In low-temperature studies²⁰ at ambient pressure, $A_g - F_g$ splitting of 0.37 cm⁻¹ was observed for the ν^- mode, while no splitting could be detected for the ν^+ mode within experimental uncertainty of 0.1 cm⁻¹.

For the orthorhombic high-pressure phase, four Raman-active librational modes with A_g , B_{1g} , B_{2g} , and B_{3g} symmetry are expected.²¹ In the vibronic region the Raman spectrum should contain the symmetric stretch mode ν^+ , split into two components A_g and B_{3g} , and due to the effect of Fermi resonance a bound state ν^- , split into A_g and B_{3g} components.²²

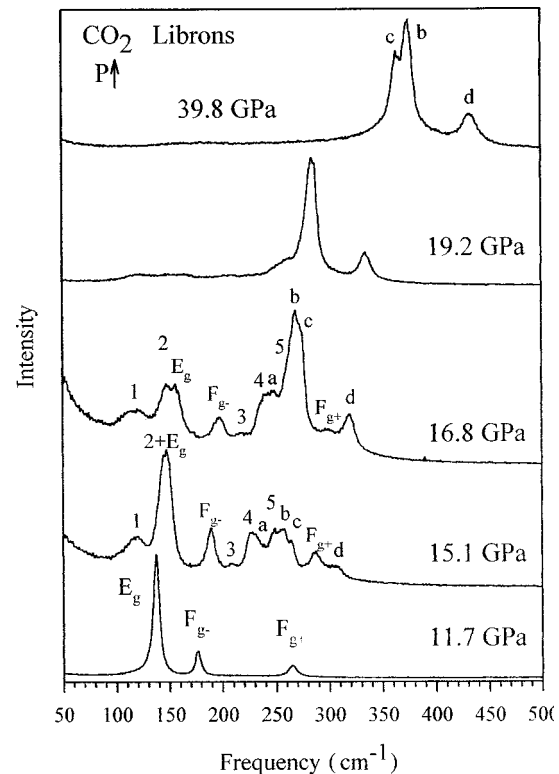


FIG. 1. Lattice mode Raman spectra of solid CO₂ at various pressures (hydrostatic run, loading cycle).

RESULTS

Librons

The evolution of spectral features with increasing pressure in the low-frequency region from the hydrostatic run are shown in Fig. 1 and can be characterized as follows: Up to ~12 GPa the three Raman-active librational modes (E_g , F_{g-} , and F_{g+}) characteristic for phase I were observed. At higher pressure new bands (3, 4, 5, a, b, c) appear with frequencies between the two librational modes of phase I with F_g symmetry and a new peak (d) on the high-frequency side of the F_{g+} mode. Furthermore splitting of the E_g mode is observed (peak 2) and an asymmetric band (peak 1) appears also on the low-frequency side of the E_g mode. Intensity changes are observed in the new bands between F_{g-} and F_{g+} mode of phase I with increasing pressure. Above ~20 GPa phase-I peaks vanish as well as some of the new ones (1, 2, 3, 4, 5) and the Raman spectra become more simple. At 39.8 GPa an intense doublet (c, b) and a weaker mode (d) at higher frequencies can be clearly distinguished. During unloading these spectral features remain preserved down to 12 GPa. Between 20 and 30 GPa the doublet (b, c) cannot be resolved, however, it is clearly present at lower pressures with the intensity ratio reversed indicating mode crossing under pressure. A further peak on the low-frequency side of the doublet and denoted by a in Fig. 2, which is difficult to recognize at higher pressures due to its low intensity, becomes more intense below 20 GPa on unloading. At 10 GPa and below, only the three modes characteristic of phase I were observed.

The spectra up to 12 GPa on loading and below 10 GPa on unloading are characteristic for cubic phase I. The spectra

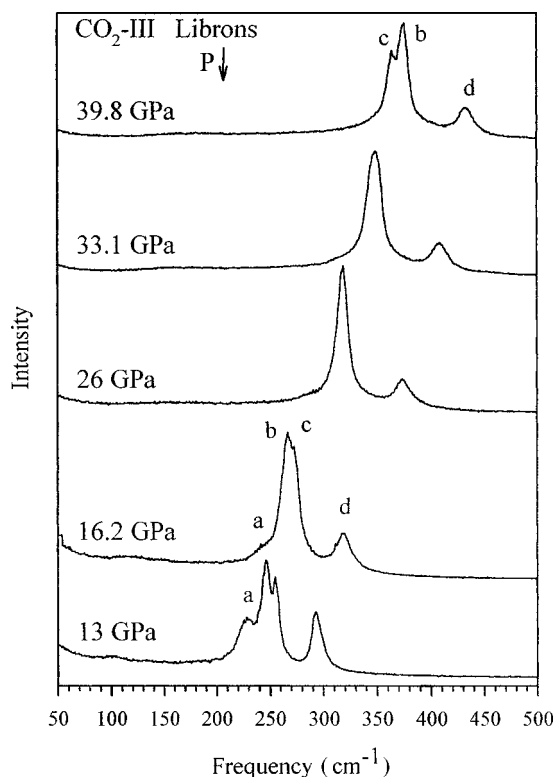


FIG. 2. Raman spectra of CO₂-III librational modes at various pressures (hydrostatic run, unloading cycle).

above ~ 20 GPa on loading and down to ~ 12 GPa on unloading consist of four modes in agreement with symmetry analysis for space group *Cmca*. The Raman spectra at 15.1 and 16.8 GPa in Fig. 1 consist of more than seven modes. In this pressure range the spectral features cannot be explained just by a mixture of the low-pressure phase I (three Raman-active modes) and high-pressure phase III (four Raman-active modes).

Increasing the the pressure for a second time into the stability field of phase III, the transition to phase III was spread over a larger pressure range. Though phase III peaks dominate at 21.5 GPa there were still low intensity peaks of the lower-pressure phases present. A spectrum typical for the first slight changes of spectral features of phase I, obtained in this second cycle, is shown in Fig. 3. The frequency positions of the four phase-III librational modes (*a*, *b*, *c*, *d*) at this pressure, which are precisely known from the downstroke run, are indicated by the vertical arrows. Besides the three modes typical of phase I, four additional bands (1, 3, 4, 5) as well as broadening of the phase I E_g mode due to splitting can be recognized. The asymmetries on the higher-frequency sides of peaks 3, 4, and 5 may indicate the presence of minor portions of phase III. The new bands (1–5) are considered as indicators for an intermediate phase IV and the spectrum of Fig. 3 indicates that phase IV appears prior to the formation of phase III. Deconvolution of the Raman spectrum at 16.8 GPa of Fig. 1 is shown in Fig. 4. In this spectrum the four modes of phase III (*a*, *b*, *c*, *d*) are the dominant features, but the three modes characteristic of phase I and five new peaks (1, 2, 3, 4, 5), which characterize phase IV, are also present.

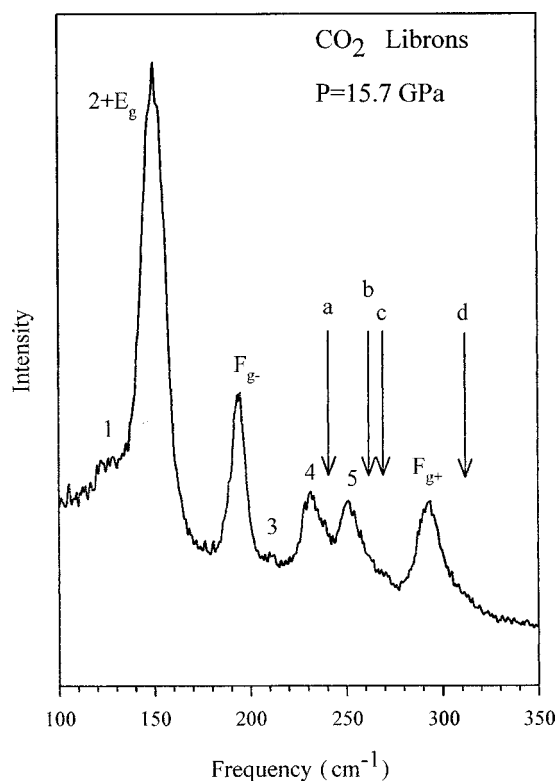


FIG. 3. Lattice mode Raman spectrum of CO₂ at 15.7 GPa (hydrostatic run, reloading cycle). The arrows indicate the frequencies of the four librational Raman modes of CO₂-III.

The pressure shifts of all low-frequency lattice modes of the hydrostatic run are shown in Fig. 5, where we have also included results from the experiments on the pure CO₂ non-hydrostatic sample. The pressure-frequency data of the observed bands are also summarized in Table I for the different loading cycles.

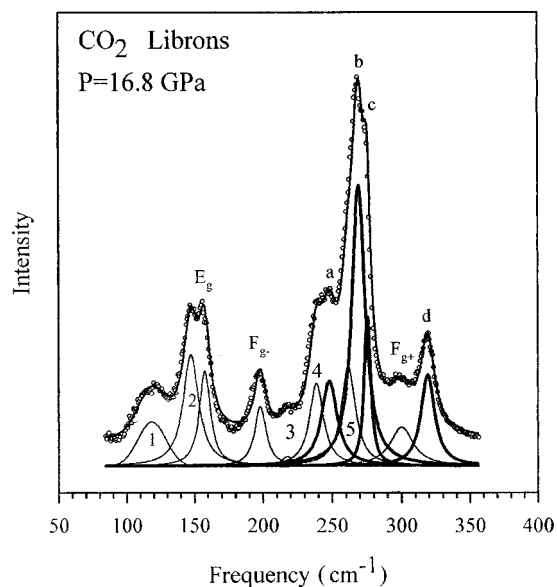


FIG. 4. Comparison of observed and fitted lattice mode Raman spectra of solid CO₂ at 16.8 GPa. Open circles indicate observed Raman spectrum; solid line through open circles indicates sum curve of the fit; the individual bands of the fit are represented by solid lines in the lower part: thick solid lines indicate CO₂-III lattice modes; thin solid lines indicate lattice modes of CO₂-I and/or CO₂-IV.

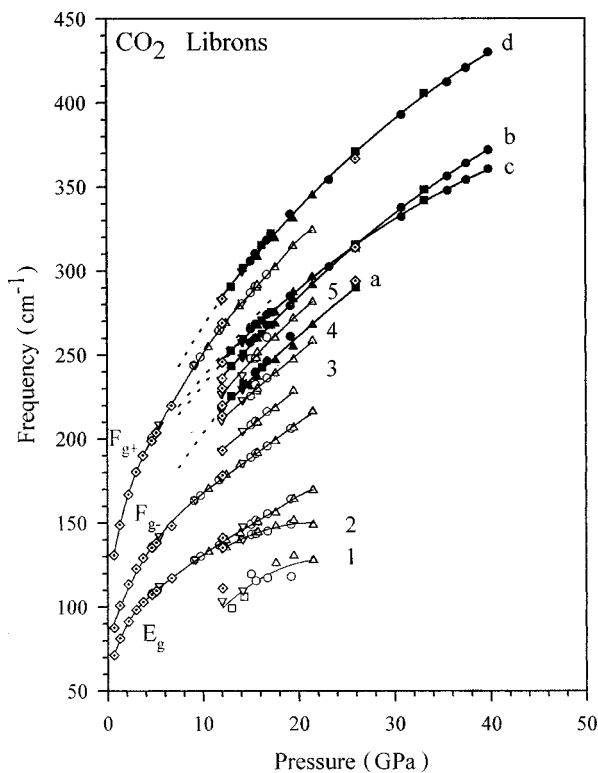


FIG. 5. Pressure shift of Raman-active lattice modes of solid CO_2 . Solid symbols indicate CO_2 -III (thick solid lines); open symbols denote CO_2 -I and CO_2 -IV (thin solid lines); circles denote the loading cycle; squares denote the unloading cycle; upward triangles indicate the reloading cycle; downward triangles indicate the re-unloading cycle. Besides all data points from the hydrostatic run data points up to 7 GPa and for 12.1 and 26 GPa from the run on pure CO_2 are also included and are shown as dotted diamonds. Dashed lines are theoretical results from Ref. 10. The solid lines serve as a guide for the eye. Note the crossing of modes *b* and *c* of CO_2 -III around 26 GPa.

Vibrons

Spectra of the Raman-active internal modes ν^+ and ν^- from the hydrostatic run are shown in Figs. 6–8. For pressures below ≈ 7 GPa the present results are in agreement with those of previous studies^{6,9} for phase I. At higher pressures some subtle changes in the spectra occur which have not been observed in previous studies. Above 9 GPa a low intensity peak (labeled with *x* in Figs. 6 and 7) can be distinguished on the high-frequency side of the ν^+ peak. Around 13 GPa another peak (labeled with *+* in Figs. 6 and 7) starts to grow up on the low-frequency side of ν^+ . In the deconvoluted spectrum at 15.1 GPa shown in Fig. 7 the three peaks can clearly be distinguished. The new band on the low-frequency side grows up in intensity with increasing pressure whereas the other two bands decrease in intensity. Above ~ 20 GPa only this new band is observed and is preserved down to 12 GPa on the unloading cycle and is assigned to phase III. The pressure shift of observed bands in the ν^+ region is shown in Fig. 9. All modes increase in frequency with increasing pressure. The frequency of ν^+ is slightly lower in phase III as compared to phase I in the observed pressure range and also exhibits a slightly smaller pressure shift. From all bands the high-frequency peak, which can be observed between 9 and 20 GPa, shows the

largest pressure shift. Reloading from 10 GPa and again unloading showed the same results with the pressure range, where all three modes coexist, shifted to higher pressures by a few GPa.

As is well known from previous experiments, ν^- decreases with increasing pressure in phase I and loses considerably in intensity due to FR, which makes it difficult to obtain satisfactory spectra in the higher pressure regime. The results of the present study show that splitting of ν^- is observed above 6.7 GPa and that two components are observed in the high-pressure phase III located a few wave numbers above the ν^- mode of phase I. A deconvoluted spectrum of the ν^- spectral region is shown in Fig. 8. The origin of the broad feature at the low-frequency side in the spectrum is not yet clear. From its frequency location, this feature might be assigned to an isotopic species, but the intensity appears too high to be in accordance with their natural abundances. The pressure shifts of the dominant lines in the ν^- region are shown in Fig. 9 up to 23 GPa. At higher pressures, the signals became very weak due to pressure tuning of Fermi resonance. The pressure-frequency data of the vibronic bands are summarized in Table II.

Liquid-to-solid transition

In the experiment on the pure CO_2 sample below 0.6 GPa the frequencies of the internal modes are a few wave numbers higher than one would expect from the extrapolated pressure shifts of the phase-I vibrons (see Fig. 10). Since in this pressure range no signals in the low-frequency region could be recorded, we infer that below 0.6 GPa CO_2 is liquid. In the mixed-gas sample CO_2 remained liquid up to 1.5 GPa on loading where we observed vibrational modes both of the liquid and solid phase. In the down stroke run signals of the solid phase could be observed down to 1.2 GPa. Both in liquid CO_2 and in the liquid CO_2 -He- N_2 mixture a rather weak band is observed around 1410 cm^{-1} on the high-frequency side of the ν^+ mode which corresponds probably to the gas-phase “hot” band at 1410 cm^{-1} reported by Stoicheff.²³

Comparison between the hydrostatic and nonhydrostatic experiments

The evolution of the spectral features in the librionic spectral region proceeds in the pure CO_2 sample in the same way as described above as pressure increases. This can be noticed in Fig. 5, where the frequencies of the librational modes observed for pure CO_2 , are shown for comparison at 12 and 26 GPa. Due to nonhydrostatic effects the corresponding changes are shifted to slightly lower pressures in the experiment on pure CO_2 . Splitting of the E_g mode can be noticed already at 9 GPa. The first new spectral features between F_{g-} and F_{g+} appeared around 10 GPa. Pure phase-III spectra could be observed at 17.8 GPa and above. On unloading pure phase-III spectra remain preserved down to 11.6 GPa and pure phase-I spectra are observed below 9 GPa. Splitting of the E_g mode is still present at 6.2 GPa during further unloading. On reloading the transition to phase-III takes place over a larger pressure range and only above 24 GPa are spectra of solely phase III observed. With the exception of larger peak widths due to the rising pressure inhomogeneities

TABLE I. Observed lattice mode frequencies of solid CO₂ in cm⁻¹.

<i>P</i> (GPa)	Phase J and phase IV							Phase III				
	1	2	<i>E_g</i>	<i>F_g⁻</i>	<i>F_g⁺</i>	3	4	5	<i>a</i>	<i>b</i>	<i>c</i>	<i>d</i>
CO ₂ with He-N ₂ as pressure transmitting medium												
4.7			108.3	136.1	200.8							
9.1	†		128.0	163.5	243.8							
9.8			130.2	166.4	248.8							
11.7			136.8	175.9	264.5							
15.1	119.7	143.1	149.3	189.2	286.9	208.3	225.5	247.8	232.0	257.3	265.3	305.7
15.6	115.7	143.7	151.7	191.4	290.7	210.5	232.5	247.9	239.8	260.0	268.3	310.3
16.8	117.4	145.2	155.5	195.9	297.8	216.2	236.2	260.5	246.4	267.7	273.9	318.1
19.2	118.2	149.3	164.3	206.2					261.0	279.3	285.0	333.8
23.3											302.4	354.1
30.8										337.6	332.2	392.9
35.6										356.3	347.7	412.3
37.5										363.9	354.1	420.7
39.8										371.9	360.6	430.0
33.1										348.3	342.0	405.8
26.0									290.2	313.6	315.6	371.2
17.2									249.5	268.0	275.4	322.2
16.2									242.7	262.6	270.6	315.4
14.3	106.2								233.0	250.5	259.5	301.7
13.0	99.4								225.6	243.5	252.7	290.5
10.6			132.9	170.4	254.8							
12.5		135.5	139.8	178.8	268.8							
13.9		139.7	144.0	184.8	278.8							
15.7		144.3	150.3	191.6	290.0	209.6	228.4	248.0			267.5	
15.8		144.6	150.9	191.9	291.5	209.9	230.0	251.5	237.0	259.7	267.4	308.0
17.6	126.2	147.9	156.2	198.8	302.1	218.4	239.0	260.2	246.8	268.4	275.2	319.4
19.5	130.5	151.6	164.3	206.7	314.8	228.6	247.2	271.5	255.0	282.9	287.1	331.1
21.5	127.8	148.8	169.6	216.3	324.2		258.4	281.4	267.8	291.4	296.4	344.8
14.2	110.1	140.3	148.2	185.8	281.3	204.8	223.2	238.1	229.9	248.6	257.7	299.8
12.0	103.7	135.3	139.5	176.8	265.7	193.0	211.1	227.0	217.2	235.2	245.7	282.7
9.2			128.3	164.0	244.1							
5.4			112.6	142.2	208.7							
CO ₂ without pressure transmitting medium												
0.6			71.1	87.2	130.5							
0.7			71.4	87.8	131.0							
1.3			81.5	101.00	149.0							
2.2			91.5	113.7	167.1							
3.0			98.5	122.9	180.5							
3.7			103.1	129.3	190.3							
4.7			107.6	135.4	199.0							
5.1			109.8	138.4	203.8							
6.7			117.3	148.5	219.9							
12.1	111.3	135.4	141.3	178.4	269.0	193.3	214	230.2	220	236.2	245.7	283.4
26									294	314		366.8

with increasing pressure the results on the pure CO₂ sample in the ν^-/ν^+ region are in agreement with those of the hydrostatic run. The agreement of the changes in the spectral features and their pressure shifts between the hydrostatic and nonhydrostatic (pure CO₂) experiments indicates that the additional spectral features (peaks 1–5) cannot be attributed to either N₂ or He forming a solid solution or van der Waals compound with CO₂. The main advantage of using the gas

mixture is that the pressure inhomogeneities are drastically reduced as compared to pure CO₂, resulting in improved resolution of the Raman spectra in the high-pressure range. Figure 11 shows phase-III Raman spectra of both runs at approximately the same pressure. In the pure CO₂ sample the Raman bands are very broad and not well resolved indicating comparatively huge pressure inhomogeneities. In addition a broad asymmetric feature is observed around 650 cm⁻¹. This

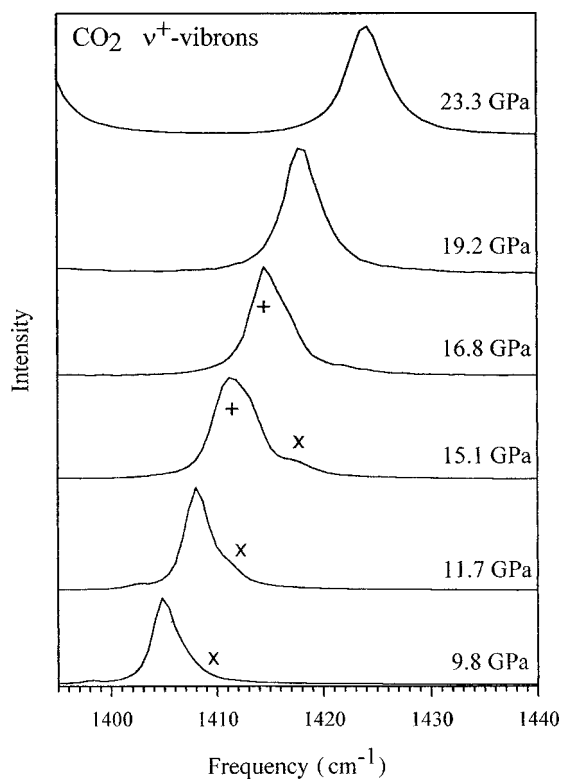


FIG. 6. Raman spectra of solid CO₂ at various pressures of the ν^+ region (hydrostatic run).

band appeared around 24 GPa during loading and remained down to 12 GPa in the unloading cycle. The asymmetry of this band indicates that it is composed of several components. In Fig. 12 the pressure shift of this band is compared with the phase-III bending mode components as determined by infrared spectroscopy.¹⁵ From the point of view of fre-

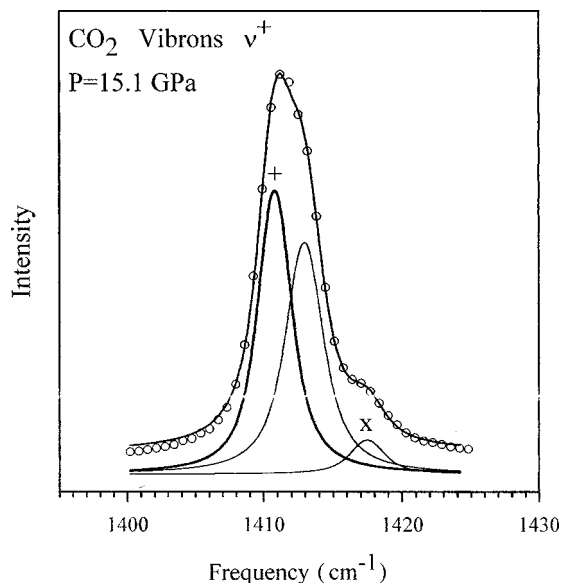


FIG. 7. Comparison of observed and fitted Raman spectra of the ν^+ region of solid CO₂ at 15.1 GPa. Open circles are the observed Raman spectrum; solid line through open circles indicates the sum curve of the fit; the individual bands of the fit are represented by solid lines in the lower part: thick solid lines indicate CO₂-III; thin solid lines indicate CO₂-I and/or CO₂-IV.

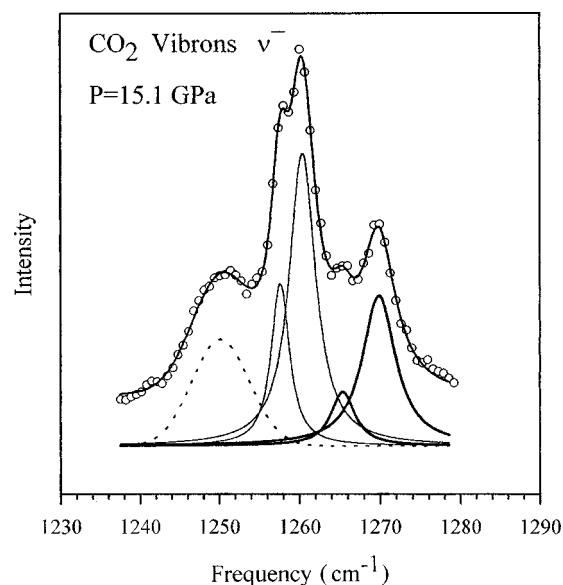


FIG. 8. Comparison of observed and fitted Raman spectra of the ν^- region of solid CO₂ at 15.1 GPa. Open circles indicate the observed Raman spectrum; solid line through open circles are the sum curve of the fit; the individual bands of the fit are represented by solid lines in the lower part: thick solid lines indicate CO₂-III; thin solid lines indicate CO₂-I and/or CO₂-IV; dashed line indicates unidentified mode.

quency and pressure shift, this band is assigned to the bending mode ν_2 of CO₂-III. The appearance of this Raman-forbidden mode is another manifestation for the existence of large uniaxial stress components in pure CO₂ at high pressures (acting as its own pressure-transmitting medium), which reduce the crystal symmetry and as a result lift the rigorous selection rules for the *Cmca* structure.

DISCUSSION

The present results on librational modes suggest that in the upstroke run for pressures above ≈ 17 –20 GPa pure phase-III Raman spectra are observed. This pressure range depends on the pressure conditions as well as on the pressure history of the sample. The pressure range in which pure phase-I Raman spectra are present extends to 10–13 GPa. Hysteresis effects are observed in the down-stroke runs. In a subsequent pressure range, 13–20 GPa, besides the three Raman bands of CO₂-I, five additional peaks, which are not characteristic of phase III can be distinguished as is demonstrated in Fig. 3. Only at higher pressures do the Raman lines of CO₂-III appear (see Figs. 1 and 4).

At this stage it is worth comparing the present results with those of the three previous high-pressure Raman studies, because they also show some of the new features found in the present study. Hanson⁸ reported the transition to phase III around 18 GPa in the upstroke run. In this paper is also shown a spectrum at 14.5 GPa, which is dominated by the three modes characteristic of phase I. However, in this spectrum one can also recognize two very low intensity signals between the two F_g modes, similar to the spectrum shown in Fig. 3. These features were observed also by Olijnyk *et al.*⁹ together with the splitting of the phase-I E_g mode which led them to speculate on the possible existence of a phase IV

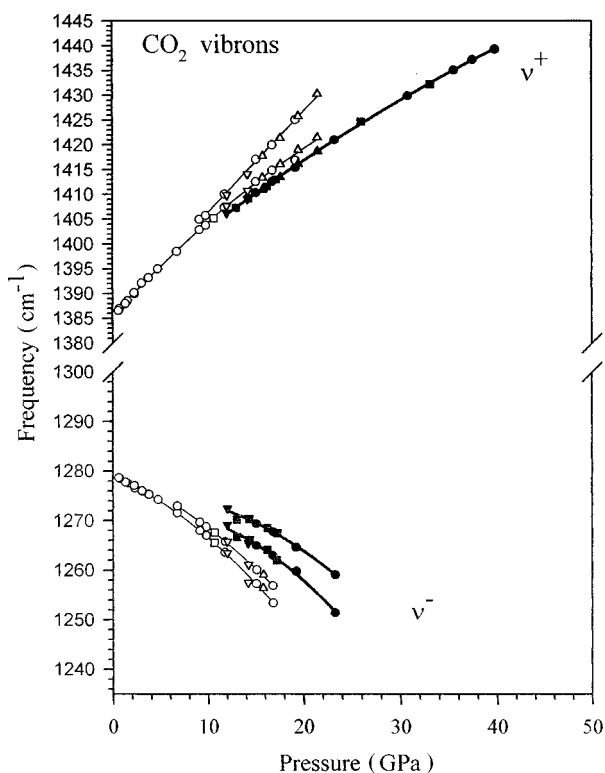


FIG. 9. Pressure shift of Raman-active modes of solid CO₂ of the ν^+/ν^- region. Solid symbols indicate CO₂-III (thick solid lines); open symbols indicate CO₂-I and CO₂-IV (thin solid lines); circles indicate the loading cycle; squares indicate the unloading cycle; upward triangles indicate the reloading cycle; downward triangles indicate the reuniting cycle. Besides all data points from the hydrostatic run data points up to 7 GPa from the run on pure CO₂ are also included. The solid lines serve as a guide for the eye.

prior to the transition to phase III. Splitting of the E_g mode can also be observed in the Raman spectrum at 19.6 GPa, shown in the paper of Aoki, Yamawaki, and Sakashita.¹³ The assignment of the mode at ≈ 250 cm⁻¹ to the F_{g+} mode of phase I in this spectrum is incorrect and comparison with the present data shows that this misinterpreted mode is better assigned to the extra mode 4 of phase IV.

The present study clearly shows that the spectral features of the librational modes in the range between 10 and 20 GPa cannot be explained just by a mixture of CO₂-I and CO₂-III. Free-energy calculations indicate that a tetragonal phase isomorphous with the $P4_2/mnm$ γ -N₂ phase is also a possible high-pressure phase.¹⁰ In this structure there are two Raman-active low-frequency modes.²⁴ A mixture of the three CO₂ structures with $Pa3$, $Cmca$, and γ -N₂ symmetry would account only for 9 of the 12 observed modes. Also no evidence for this tetragonal phase has been found by x-ray diffraction.¹⁴ One striking feature of the librational spectra in this intermediate pressure range is that all peaks characteristic of phase I including those of the new peaks which do not belong to phase III persist up to the pressure above which solely phase-III peaks are observed. The observed splitting of the phase-I E_g mode suggests a small distortion of the cubic lattice, e.g., but not necessarily, to a tetragonal or an orthorhombic lattice. Though the x-ray-diffraction pattern of CO₂ at 11.8 GPa has been interpreted in terms of a mixture of cubic and orthorhombic phases,¹⁴ some evidence can be

found from this study that the cubic symmetry of phase I is lost in the phase mixture regime. In Fig. 2 of Ref. 14, observed and calculated diffraction patterns are compared. In the observed pattern there is a diffraction peak at $2\theta \approx 16.3^\circ$, which is not assigned to any phase. The 200 diffraction reflection of cubic phase I should occur at a smaller value $2\theta \approx 16^\circ$, as can be seen also in the calculated pattern. For a tetragonal distortion this would imply a change of the c/a ratio from 1 to 0.98.

Usually one peak is observed at ν^+ and ν^- at high pressures in phase I due to small A_g - F_g splitting. Within the framework of cubic phase I the two components, which can be distinguished for both modes above 9 and 7 GPa, respectively, in phase I, must be assigned to the A_g and F_g components of the bound states. Between 10 and 20 GPa splitting of the ν^+ mode increases from 2 to 7 cm⁻¹ whereas it is smaller for ν^- . Since theoretical studies²⁵ confirm that A_g - F_g splitting is very small in the pressure range up to 10 GPa for the cubic phase, though no numbers have been given, the quite large frequency difference of the ν^+ components might be regarded as another hint that cubic symmetry is lifted in this pressure range.

From recent spectroscopic studies^{9,13,15} of the *internal* modes no indications for the existence of the intermediate phase IV have been found. Also in the present study no clear-cut indications for phase IV could be noticed in the spectra of the *internal* modes. In view of the subtle nature of the I→IV transition, which apparently involves only slight modifications of the cubic $Pa3$ structure, it might not be surprising that the internal modes are affected only very weakly by this transition. A careful x-ray-diffraction study is necessary to determine which structures beside $Cmca$ are present in the mixed phase regime.

The $Cmca$ structure of the high-pressure phase III allows four Raman modes. In the present study three modes of this phase are observed clearly in the loading run above 20 GPa and the fourth mode can clearly be distinguished in the unloading run below 20 GPa as well as in the regime of phase mixtures using deconvolution techniques. These results indicate that the intensity of this mode is rather low and decreases with increasing pressure. Similar effects have been observed also in other molecular solids crystallizing in the $Cmca$ structure: For N₂O only two broad bands could be observed in the $Cmca$ phase,²⁶ which, besides the effect of pressure inhomogeneities, is the result of molecular disorder, which manifests itself in line broadening so that the the four peaks cannot be resolved even at low temperatures. For CS₂ (Ref. 27) and C₂H₄ (Ref. 28) three librational bands out of four have been observed in the investigated pressure range. In the case of the halogens very small intensities have been observed for the two lowest-lying librational modes.²⁸⁻³²

For CS₂ (Ref. 27) and C₂H₄ (Ref. 28) crossing of the two lowest frequency librations has been observed with increasing pressure. For CO₂-III crossing occurs for the two intermediate modes. One might speculate that the modes involved in crossing have the same symmetry in all three substances. Unfortunately there is no definite symmetry assignment of the librational modes for these substances.

Calculated values of the librational mode frequencies have been given for the pressure range between 7 and 18 GPa.¹⁰ There is excellent agreement for the lowest and high-

TABLE II. Observed vibronic frequencies of solid CO₂ in cm⁻¹.

<i>P</i> (GPa)	Phase I and phase IV				Phase III		
	ν^-	ν^+	ν^-	ν^+			
CO ₂ with He-N ₂ as pressure transmitting medium							
4.7	1274.3		1395.0				
9.1	1268.0	1269.7	1402.9	1405.0			
9.8	1267.0	1268.8	1403.8	1405.8			
11.7	1263.6	1265.8	1407.4	1410.1			
15.1	1257.3	1260.1	1412.6	1417.1	1265.0	1269.4	1410.4
16.8	1253.4	1256.9	1414.9	1420.0	1263.0	1267.8	1412.6
19.2			1416.9	1425.1	1259.8	1264.6	1415.4
23.3					1251.4	1259.1	1421.0
30.8							1429.9
35.6							1435.1
37.5							1437.2
39.8							1439.3
33.1							1432.2
26.0							1424.7
17.2					1262.0	1267.5	1413.0
16.2					1264.1	1268.5	1411.6
14.3					1266.1	1270.3	1409.2
13.0					1266.7	1270.2	1407.3
10.6	1265.5	1267.6	1405.2	1407.9			
15.8	1256.4	1259.1	1413.4	1417.8			1411.0
17.6			1416.1	1421.4			1413.5
19.5			1419.0	1425.8			1416.2
21.5			1421.5	1430.3			1418.7
14.2	1257.5	1261.2	1410.8	1414.1	1265.5	1270.6	1409.1
12.0	1263.5	1265.8	1407.7	1409.9	1269.2	1272.5	1406.3
1.5	1277.6		1388.6				
2.3	1276.6		1390.0				
CO ₂ without pressure transmitting medium							
6.7	1271.6	1273.0	1398.5				
3.7	1275.3		1393.2				
3.0	1276.0		1392.2				
2.2	1277.1		1390.2				
1.3	1277.8		1388.0				
0.7	1278.6		1387.0				
0.6	1278.7		1386.6				

est frequency mode. At least one of the two intermediate modes is not well described by these calculations and may be regarded as another indication that refinements of the intermolecular model potential are necessary to reproduce the experimental results correctly.

In the orthorhombic phase III there should be two Raman-active components of A_g and B_{3g} symmetry for ν^+ and ν^- . From observed ν_3 and $(\nu_1 + \nu_3)$ combination Lu and Hofmeister¹⁵ calculated two components for the symmetric stretch mode ν_1 separated by 75 cm⁻¹ in the pressure range 10–15 GPa. This higher-frequency component has frequency values quite similar to the high-frequency Raman peak observed between 9 and 20 GPa in the ν^+ region, but we would like to emphasize that this Raman peak is definitely representative for one of the low-pressure phases and not for *Cmca* phase, because it is not observed in the unloading cycle, where phase III could be retained down to ~12 GPa.

Since Fermi resonance is not present in the IR overtones³³ these calculated ν_1 bands should represent the undisturbed modes and are not comparable to the present ν^+ results. At those pressures where exclusively librations of phase III are present, we observe one peak in the ν^+ frequency range and two bands in the ν^- region. For ν^+ either the separation of A_g and B_{3g} is too small or one component has a too small intensity to be detectable in our experiments. In the ν^- region the higher-frequency component is tentatively assigned to A_g and the lower-frequency component to B_{3g} as in the case of CS₂. The separation between both components increases from ≈ 4 cm⁻¹ at 12 GPa to ≈ 6 cm⁻¹ at 20 GPa. Splittings of comparable magnitude have been observed for solid CS₂, another three-atomic molecule, which also crystallizes in the *Cmca* lattice.²²

Based on IR studies of vibrons of CO₂ imbedded in argon, Lu and Hofmeister¹⁵ proposed that at room temperature the

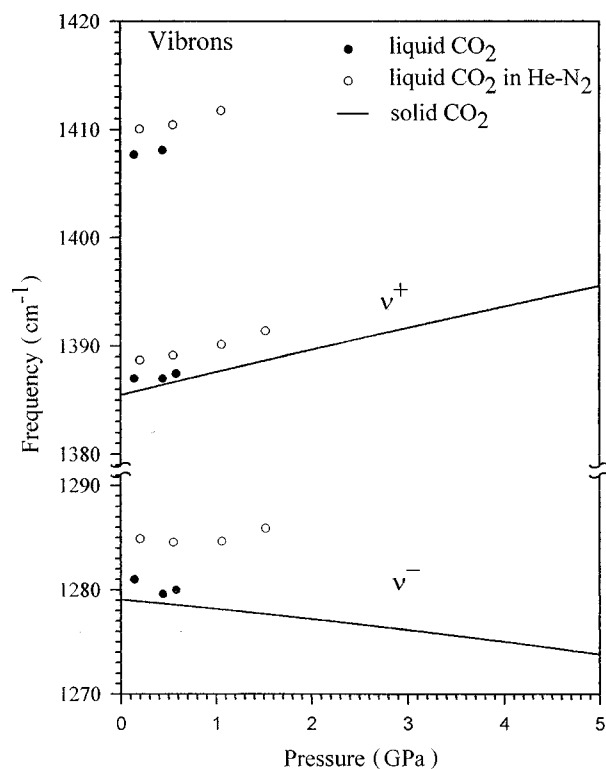


FIG. 10. Pressure shift of Raman-active ν^+ and ν^- modes of solid and liquid CO₂. Solid lines are solid CO₂; solid circles are liquid CO₂; open circles are liquid CO₂ in N₂-He.

gas-to-liquid transition occurs near 0.6 GPa and the liquid-to-solid transition occurs in the vicinity of 2 GPa. The present study clearly shows that CO₂ undergoes the liquid-to-solid transition near 0.6 GPa at room temperature as determined previously¹⁻³ and that there is really no need for a revision of that part of the phase diagram of CO₂. The effect of admixing He-N₂ or Ar shows up in a shift of the liquid-

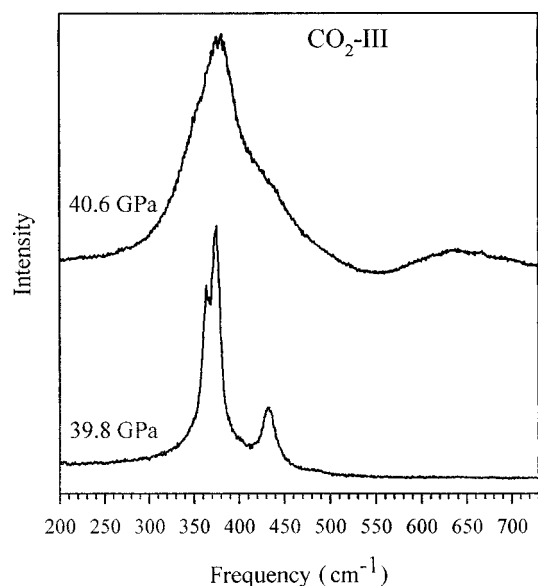


FIG. 11. Comparison of Raman spectra of CO₂-III at around 40 GPa. Upper spectrum show, pure CO₂; lower spectrum show, CO₂ with N₂-He as pressure transmitting medium.

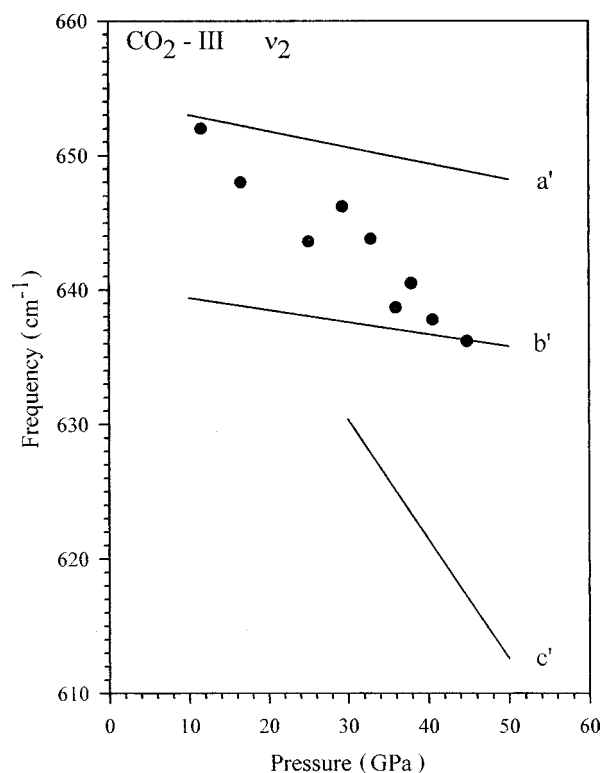


FIG. 12. Pressure shift of the bending mode ν_2 in CO₂-III. Solid lines indicate ν_2 components from infrared spectroscopy (Ref. 15); solid circles indicate the position of the center-of-mass of the band observed by Raman spectroscopy.

solid transition to higher pressures, which has been well known, for example, in the system N₂-He.³⁴ The effect of the admixed components manifests itself in a decrease of some contributions to the intermolecular potential, which make it effectively weaker resulting in higher liquid-solid transition pressures.³⁵

CONCLUSIONS

In this paper we have reported on the results of high-pressure Raman studies on CO₂ under hydrostatic and non-hydrostatic pressure conditions. In contrast to the widely adopted view that solid CO₂ transforms directly from phase I to phase III between 10 and 20 GPa, the pressure changes of the librational spectra indicate the formation of an intermediate phase IV prior to the transition to phase III. Taking into account the results of a recent x-ray-diffraction study the present Raman results suggest that the structure of phase IV is a slight distortion of the cubic phase I. The observation that the transition to phase IV is not easily detected in the vibrational modes, may be taken as another indication for the subtlety of this phase transition. In the stability field of phase I, we have reported factor-group splitting in the ν^+ and ν^- modes. The effect of pressure on all four Raman-active librations of phase III has been documented over a wide pressure range. Crossing of two librational modes occurs with increasing pressure, and is similar to the behavior in CS₂ and

C₂H₂. In phase III, the ν^+ mode has a slightly lower frequency and the ν^- mode has slightly higher frequency than in the preceding phase. The liquid-to-solid transition pressure of 0.6 GPa in CO₂ is confirmed.

ACKNOWLEDGMENT

Support for this project was provided in part by the European Community under Contract No. SCI*CT920802.

-
- ¹P. W. Bridgeman, Proc. Am. Acad. Arts Sci. **72**, 207 (1938).
²J. D. Grace and G. C. Kennedy, J. Phys. Chem. Solids **28**, 977 (1967).
³H. Shimizu, T. Kitagawa, and S. Sasaki, Phys. Rev. B **47**, 11 567 (1993).
⁴L. Liu, Nature (London) **303**, 508 (1983).
⁵B. Olinger, J. Chem. Phys. **77**, 6255 (1982).
⁶R. C. Hanson and L. H. Jones, J. Chem. Phys. **75**, 1102 (1982).
⁷L. Liu, Earth Planet. Sci. Lett. **71**, 104 (1984).
⁸R. C. Hanson, J. Phys. Chem. **89**, 4499 (1985).
⁹H. Olijnyk, H. Daeufer, H.-J. Jodl, and H. D. Hochheimer, J. Chem. Phys. **88**, 4204 (1988).
¹⁰B. Kuchta and R. D. Ethers, Phys. Rev. B **38**, 6265 (1988).
¹¹R. D. Ethers and B. Kuchta, J. Chem. Phys. **90**, 4537 (1989).
¹²B. Kuchta and R. D. Ethers, Phys. Rev. B **47**, 14 691 (1993).
¹³K. Aoki, H. Yamawaki, and M. Sakashita, Phys. Rev. B **48**, 9231 (1993).
¹⁴K. Aoki, H. Yamawaki, M. Sakashita, Y. Gotoh, and K. Take-mura, Science **263**, 356 (1994).
¹⁵R. Lu and A. M. Hofmeister, Phys. Rev. B **52**, 3985 (1995).
¹⁶A. P. Jephcoat, H.-K. Mao, and P. M. Bell, in *Hydrothermal Experimental Techniques*, edited by G. C. Ulmer and H. L. Barnes (Wiley Interscience, New York, 1987), p. 469.
¹⁷H. K. Mao, J. Xu, and P. M. Bell, J. Geophys. Res. **91**, 4673 (1986).
¹⁸A. Anderson and T. S. Sun, Chem. Phys. Lett. **8**, 537 (1971).
¹⁹F. Bogani and P. R. Salvi, J. Chem. Phys. **81**, 4991 (1984).
²⁰R. Ouillon, P. Ranson, and S. Califano, J. Chem. Phys. **83**, 2162 (1985).
²¹A. Anderson, P. J. Grout, J. W. Leech, and T. S. Sun, Chem. Phys. Lett. **21**, 9 (1973).
²²P. Ranson, R. Ouillon, B. Perrin, and J.-P. Lemaistre, J. Chem. Phys. **96**, 6348 (1992).
²³B. P. Stoicheff, Can. J. Phys. **36**, 218 (1958).
²⁴M. M. Thiery, D. Fabre, M. Jean-Louis, and H. Vu, J. Chem. Phys. **59**, 4559 (1973).
²⁵G. Cardini, P. R. Salvi, and V. Schettino, J. Chem. Phys. **91**, 3869 (1989).
²⁶H. Olijnyk, H. Daeufer, M. Rubly, H.-J. Jodl, and H. D. Hochheimer, J. Chem. Phys. **93**, 45 (1990).
²⁷F. Bolduan, H. D. Hochheimer, and H. J. Jodl, J. Chem. Phys. **84**, 6997 (1986).
²⁸K. Aoki, Y. Kakudate, M. Yoshida, S. Usaba, K. Tanaka, and S. Fujiwara, Solid State Commun. **64**, 1329 (1987).
²⁹O. Shimomura, K. Takemura, and K. Aoki, in *High Pressure in Research and Industry*, edited by C. M. Backman, T. Johansson, and L. Tegner, *Proceedings of the 8th AIRAPT and 19th EHPRG Conference* (Arkitektkopia, Uppsala, 1982) p. 272.
³⁰P. G. Johannsen and W. B. Holzapfel, J. Phys. C **16**, L1177 (1983).
³¹P. G. Johannsen and W. B. Holzapfel, J. Phys. C **16**, 1961 (1983).
³²H. Olijnyk, W. Li, and A. Wokaun, Phys. Rev. B **50**, 712 (1994).
³³D. A. Dows and A. Schettino, J. Chem. Phys. **58**, 5009 (1973).
³⁴W. L. Vos and J. A. Schouten, Phys. Rev. Lett. **64**, 898 (1990).
³⁵M. I. M. Scheerboom, J. P. Michels, and J. A. Schouten, J. Chem. Phys. **104**, 9388 (1996).